IOPscience iopscience.iop.org

Home Search Collections Journals About Contact us My IOPscience

Contribution of the buffer layer to the Raman spectrum of epitaxial graphene on SiC(0001)

This article has been downloaded from IOPscience. Please scroll down to see the full text article.

2013 New J. Phys. 15 043031

(http://iopscience.iop.org/1367-2630/15/4/043031)

View the table of contents for this issue, or go to the journal homepage for more

Download details:
IP Address: 158.64.77.122
The article was downloaded on 22/08/2013 at 13:20

Please note that terms and conditions apply.

New Journal of Physics
The open access journal for physics

Contribution of the buffer layer to the Raman spectrum of epitaxial graphene on SiC(0001)

F Fromm[1], M H Oliveira Jr[2], A Molina-Sánchez[3,4], M Hundhausen[1], J M J Lopes[2], H Riechert[2], L Wirtz[3,4] and T Seyller[5]

[1] Lehrstuhl für Technische Physik, Universität Erlangen-Nürnberg, Erwin-Rommel-Strasse 1, D-91058 Erlangen, Germany
[2] Paul-Drude-Institut für Festkörperelektronik, Hausvogteiplatz 5-7, D-10117 Berlin, Germany
[3] Physics and Material Sciences Research Unit, University of Luxembourg, Campus Limpertsberg, L-1511 Luxembourg, Luxembourg
[4] Department of ISEN, Institute for Electronics, Microelectronics, and Nanotechnology (IEMN), CNRS UMR 8520, F-59652 Villeneuve d'Ascq Cedex, France
[5] Institut für Physik, Technische Universität Chemnitz, Reichenhainer Straße 70, D-09126 Chemnitz, Germany
E-mail: thomas.seyller@physik.tu-chemnitz.de

New Journal of Physics **15** (2013) 043031 (11pp)
Received 16 November 2012
Published 18 April 2013
Online at http://www.njp.org/
doi:10.1088/1367-2630/15/4/043031

Abstract. We report a Raman study of the so-called buffer layer with $(6\sqrt{3} \times 6\sqrt{3})R30^\circ$ periodicity which forms the intrinsic interface structure between epitaxial graphene and SiC(0001). We show that this interface structure leads to a non-vanishing signal in the Raman spectrum at frequencies in the range of the D- and G-band of graphene and discuss its shape and intensity. *Ab initio* phonon calculations reveal that these features can be attributed to the vibrational density of states of the buffer layer.

S Online supplementary data available from stacks.iop.org/NJP/15/043031/mmedia

Content from this work may be used under the terms of the Creative Commons Attribution 3.0 licence. Any further distribution of this work must maintain attribution to the author(s) and the title of the work, journal citation and DOI.

© IOP Publishing Ltd and Deutsche Physikalische Gesellschaft

Contents

1. Introduction

Raman spectroscopy is a very powerful tool for investigating carbon materials and is intensively used for the characterization of graphene obtained by different methods [1]. For example, Raman spectroscopy has been shown to be extremely useful for discerning monolayers from bilayers and multilayers [2, 3]. Furthermore, this technique provides information about the carrier concentration in graphene [4], the edges of graphene flakes [5–7] and about the properties of graphene nano ribbons [8–10]. Hence it is no surprise that it is also used to investigate epitaxial graphene grown on silicon carbide [11–23].

The Raman spectrum of graphene usually shows three main features: the D-band at around 1355 cm^{-1}, the G-band at about 1580 cm^{-1} and the 2D-band at approximately 2680 cm^{-1}. However, Raman spectroscopy is not a surface-sensitive method and usually the probed sample volume is much larger, i.e. deeper, than the graphene sheet itself. This leads to the presence of substrate-related features in the spectrum as well. For many substrates such as SiO_2/Si this is not a problem because these features do not overlap with the graphene signals. This is different for epitaxial graphene grown on SiC where the Raman spectrum in the D- and G-range is dominated by the two-phonon modes of the SiC substrate [12]. As an example, we show in figure 1(a) the Raman spectrum of hydrogen-etched 6H-SiC (see also online supplementary data available from stacks.iop.org/NJP/15/043031/mmedia). The region between around 1000 and 2000 cm^{-1} is dominated by two-phonon processes. Therefore, it has become common to correct the spectra of epitaxial graphene on SiC by subtracting the spectrum of the bare substrate. This procedure, however, assumes that the spectrum contains only contributions from the epitaxial graphene and from the SiC bulk. In the case of epitaxial graphene on SiC(0001) this assumption, however, may not be correct because it is known that the graphene sheet resides on the so-called buffer layer [24, 25]. It is nowadays widely accepted that the buffer layer itself is a graphene-like honeycomb lattice of carbon atoms on top of an otherwise unreconstructed Si(0001) surface [24, 25]. The buffer layer shows the undistorted σ-states of graphene but a distorted π-band. The distortions are caused by hybridization of the π-states with the states of the SiC(0001) surface and by the formation of covalent bonds between some of the graphene–carbon atoms and the underlying silicon atoms. Several theoretical studies have investigated various aspects of this structure, all in good agreement with experimental results [26–30]. It is natural to ask: what is the contribution of the buffer layer to the total Raman spectrum measured from epitaxial graphene on SiC? In this paper, we will show that the buffer layer leads to a non-negligible contribution in the Raman spectrum, and we will discuss the origin of the signal.

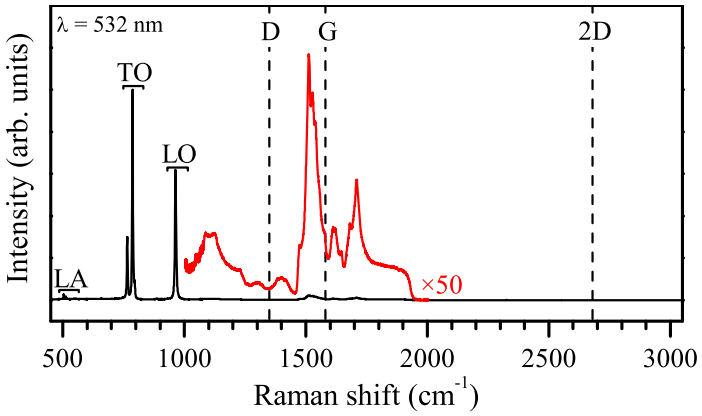

Figure 1. Raman spectrum of 6H-SiC measured with a laser wavelength of 532 nm. The signals due to the longitudinal acoustic (LA), transverse optical (TO) and longitudinal optical (LO) phonon modes are indicated. The region between 1000 and 2000 cm^{-1} is also shown after multiplication by a factor of 50. In this region, the signals due to two-phonon processes are visible. Three-phonon processes are very weak and can be neglected. The positions of the D, G and 2D lines of graphene are indicated by the vertical dashed lines.

2. Experimental details

In order to identify the contribution of the buffer layer to the Raman signal of epitaxial graphene we have studied different samples. The structures of the samples are depicted schematically in figure 2. All samples were prepared on chips cut from nitrogen-doped, on-axis oriented 6H-SiC(0001) wafer purchased from SiCrystal AG. Despite the fact that the wafer had an epi-ready chemo-mechanical polish, the surfaces were treated with an additional hydrogen etch in 1 bar H_2 at 1500 °C [31]. Samples covered with the buffer layer ($6\sqrt{3}$ for short, see figure 2(a)) were prepared by annealing the SiC(0001) sample in 1 bar Ar at $T = 1450$ °C [31]. Monolayer graphene on the buffer layer (termed MLG, see figure 2(b)) was obtained by annealing the SiC substrate in 1 bar Ar at 1650 °C [21, 31]. From previous studies it is known that such samples may contain inclusions of bilayer graphene (BLG) at positions close to the step edges [21]. Therefore, our micro-Raman spectroscopy measurements (see below) also allowed us to obtain Raman spectra from BLG on the buffer layer (see figure 2(c)). Finally, quasi-free-standing graphene on hydrogen-saturated SiC(0001) [19, 32–34] (QFMLG; see figure 2(d)) was obtained by annealing samples covered by the buffer layer in 1 bar hydrogen [19]. Reference spectra of 6H-SiC were obtained from a hydrogen-etched sample which is free of any carbonaceous surface layer.

The samples prepared in the above-mentioned ways were thoroughly characterized by x-ray photoelectron spectroscopy and atomic force microscopy. Micro-Raman spectroscopy measurements were made using a Jobin Yvon T64000 triple spectrometer combined with a liquid nitrogen-cooled CCD detector. A frequency doubled Nd:YVO_4 laser with a wavelength of 532 nm was employed. Additional spectra were measured using an Ar ion laser providing wavelengths of 476 and 514 nm. The laser beam was focused onto the sample by a 100× objective with numerical aperture NA = 0.9 and the scattered light was detected in

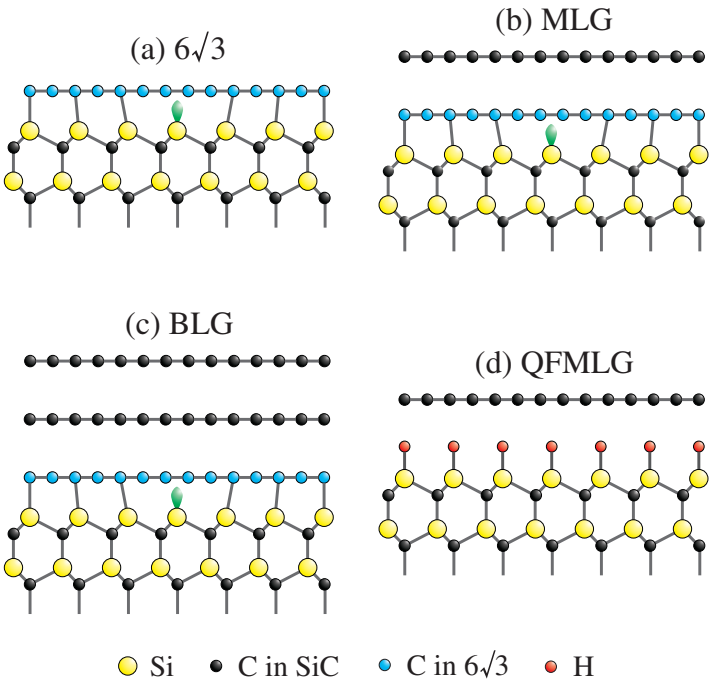

Figure 2. Schematic structures (side view) of the samples used in the present study. (a) The buffer layer ($6\sqrt{3}$) with $(6\sqrt{3} \times \sqrt{3})R30^\circ$ periodicity. (b) Monolayer graphene (MLG) situated on the buffer layer. (c) Bilayer graphene (BLG) situated on top of the buffer layer. (d) Quasi-free-standing monolayer graphene (QFMLG) on top of the hydrogen-saturated SiC surface. The carbon atoms of the buffer layer are plotted in blue.

backscattering geometry. The laser spot size was 1 μm. Unless otherwise stated, the Raman spectra were measured under the same conditions. The raw data were normalized to the maximum of the TO phonon mode of 6H-SiC at about 780 cm^{-1}.

3. Results and discussion

Figure 3(a) compiles typical Raman spectra of the different samples described above. The spectra were collected at a laser wavelength of 532 nm. The lowest spectrum (labeled $6\sqrt{3}$) was measured on the sample covered by the buffer layer. At low energies that spectrum contains two rather broad features, one centered at around 1355 cm^{-1} and the other at 1580 cm^{-1}. The latter is accompanied by a smaller peak at the low-energy side situated at around 1485–1490 cm^{-1}. No 2D line is observed for the buffer layer.

The spectra of MLG and BLG are also displayed in figure 3(a). Both spectra exhibit a G line and a 2D line. The 2D line of MLG at 2706 cm^{-1} is very well described by a single Lorentzian with a full-width at half-maximum of 35 cm^{-1}, which agrees with the notion that the sample is covered mainly by monolayer epitaxial graphene. The shape of the 2D band of BLG in figure 3(a) is consistent with what has been observed previously on both exfoliated graphene [2, 3] and epitaxial graphene [12]. Note that in this work, we are not interested in the exact positions of the G and 2D bands, which might be influenced by strain and charge. For a

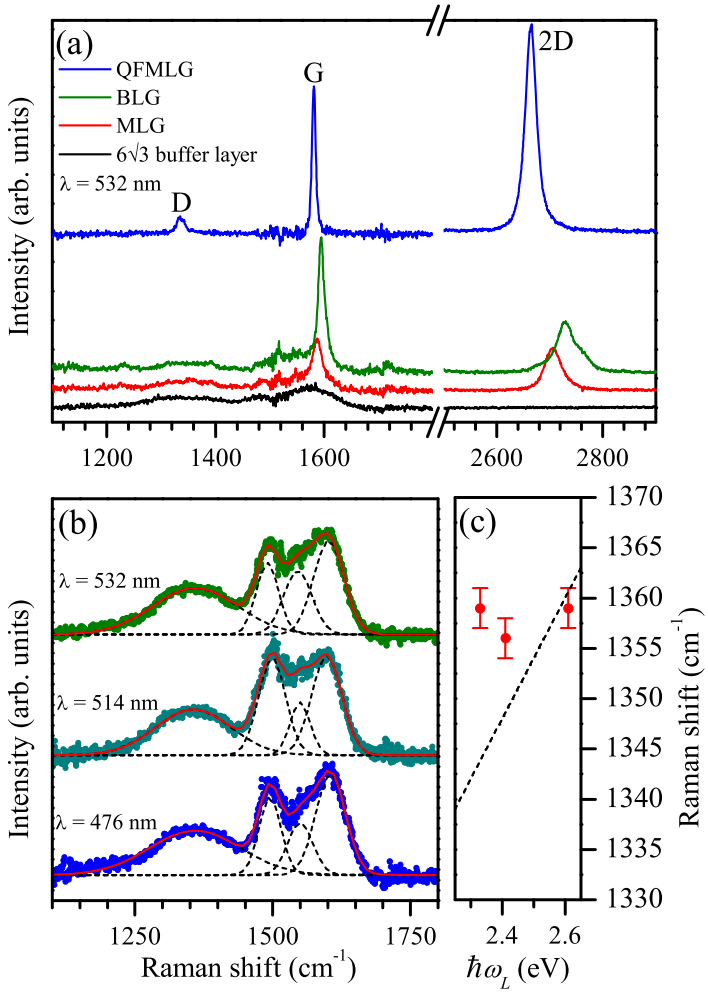

Figure 3. (a) Raman spectra of (from bottom to top) the buffer layer ($6\sqrt{3}$), MLG on the buffer layer, BLG on the buffer layer and QFMLG on H-terminated SiC(0001). The spectra were measured with a laser wavelength of 532 nm. (b) Raman spectra of the buffer layer measured with three different laser energies together with the results from a peak fitting using four components. (c) Position of the broad band at approximately 1355 cm^{-1} (red dots) for different laser photon energies compared to the dispersion (dashed line) of the D-band [51].

discussion of this topic, see previous published works [12–17, 19]. However, what is important to the present work is the observation that the spectra of MLG and BLG contain the same broad features between 1200 and 1665 cm^{-1} that are observed for the $6\sqrt{3}$ sample. Finally, figure 3(a) also shows the spectrum of a sample of QFMLG, i.e. a layer of graphene on SiC(0001) without the buffer layer at the interface. The spectrum consists of three narrow lines: the D line, the G line and the 2D line, as discussed in a previous work [19]. In contrast to the spectra of MLG and BLG, the broad features between 1200 and 1665 cm^{-1} are absent and the spectrum is basically flat between D and G lines.

This fact provides an important input. As mentioned above, the spectra shown are difference spectra where the spectrum of a clean SiC sample is subtracted from that of the

graphene-covered one. One could therefore think that the broad features described above are the result of an insufficient background correction. This is clearly ruled out by the fact that the spectrum of QFMLG, which was obtained in exactly the same way as those of the $6\sqrt{3}$, MLG and BLG samples, does not show these features. The only effect of the background subtraction is the increase of noise on both sides of the G line which can be seen in all spectra. This can be understood by considering that at those frequencies the intensity in both data sets, the one of the sample with graphene and the one used for background subtraction, is particularly large due to the contribution of the SiC substrate (see figure 1). The larger intensity at these frequencies leads to a larger statistical noise ($\sqrt{n}$ with n being the count rate) which, of course, is not removed by the subtraction of the spectra. Therefore, we can safely state that the spectrum labeled $6\sqrt{3}$ in figure 3 is the true Raman spectrum of the buffer layer which exists at the interface between SiC(0001) and epitaxial graphene.

Figure 3(b) shows three Raman spectra of the buffer layer measured with three different laser wavelengths of 476, 514 and 532 nm, which correspond to excitation energies of 2.60, 2.41 and 2.33 eV, respectively. Since the scattering intensity is zero for wavenumbers larger than approximately 1665 cm^{-1}, we show only the low-energy part of the spectrum between 1100 and 1800 cm^{-1}. The graph includes the result of a peak fitting using a total of four components for the shown frequency range. The spectra are well reproduced by the peak fitting. Figure 3(c) displays the position of the broad peak at 1355 cm^{-1} as a function of laser photon energy in comparison to the expected dispersion of the graphene D-band [51]. While the latter shows a clear dispersion of 60 $cm^{-1}\,eV^{-1}$, the broad peak of the buffer layers stays at a constant frequency. The same statement can be made about the other maxima observed in the Raman spectrum.

The Raman spectra shown in figure 3(b) do not seem to be composed of discrete peaks but rather resemble a vibrational density of states (vDOS). This is plausible since the unit cell of the $(6\sqrt{3} \times 6\sqrt{3})R30^\circ$ reconstruction is quite large and the corresponding reciprocal unit cell is small. Thus, a large part of the phonon dispersion is folded back onto Γ and becomes potentially Raman active. To a good approximation, one may therefore assume that the Raman spectra of figure 3(b) correspond to the vDOS of the buffer layer. We have verified this hypothesis by an explicit calculation of the phonon dispersion and vDOS of the buffer layer using *ab initio* methods as presented in the following.

Since the unit cell of the $(6\sqrt{3} \times 6\sqrt{3})R30^\circ$ reconstruction (and even of the recently proposed (5×5) superstructure [35]) is prohibitively large for *ab initio* calculations of phonons, we have chosen to work with the $(\sqrt{3} \times \sqrt{3})R30^\circ$ reconstruction which was also used in the electronic structure calculations of [26–29]. The model has been shown to lead to good qualitative agreement with experimental data. The unit cell for our simulation of the buffer layer on SiC is shown in figure 4. With respect to free-standing graphene, it corresponds to a (2×2) unit cell, containing eight carbon atoms. With the aim of obtaining reliable results for the phonons of the buffer layer, the commensurability between the buffer layer and SiC is obtained by squeezing the substrate by 8%, adopting the experimental lattice constant of graphene (2.46 Å). (This is different from the procedure in [26–29] where the lattice constant of graphene was increased by 8% in order to match the experimental lattice constant of SiC.) The SiC substrate is simulated by four atomic layers (two Si layers and two C layers), passivated with hydrogen atoms at the bottom. Note that in this configuration two of the eight carbon atoms of the buffer layer are on top of the silicon atoms, forming a covalent bond. The atomic positions inside the unit cell have been calculated with density functional theory (DFT) [36, 37],

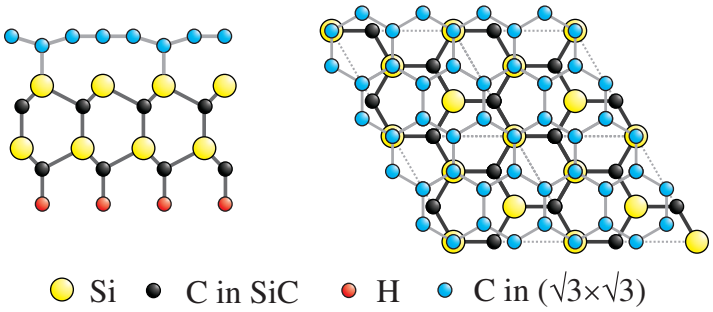

Figure 4. The unit cell used in the simulation of the buffer layer. The carbon atoms of the buffer layer are plotted in blue. For clarity, the top view shows only atoms of the topmost SiC bilayer. Hydrogen atoms passivate the dangling bonds of the carbon atoms of SiC at the bottom. In this configuration two carbon atoms of the buffer layer are on the top of silicon atoms. The drawing is not to scale.

in the local density approximation (LDA)[6]. The calculations were performed with the quantum-Espresso code [38] using ultra-soft Vanderbilt pseudopotentials, a $12 \times 12 \times 1$ k-point grid, and energy cutoff of 35 Ryd. Due to the formation of covalent bonds, the carbon atoms on top of surface Si atoms display an inward buckling by $\Delta z = 0.39$ Å (see figure 4). The distance between the other carbon atoms and the surface–Si plane is $d = 2.02$ Å.

Starting from the optimized geometry, we use density functional perturbation theory [39, 40] to calculate the phonon dispersion of the buffer layer. The result is shown in figure 5, where we have concentrated on the frequency range above 1200 cm^{-1}, which is important for the interpretation of the spectra in figure 3(b). The broad blue lines correspond to the modes of the buffer layer. (The SiC bulk modes have frequencies below 1200 cm^{-1}.) For comparison, we have included the phonon bands of isolated graphene in a 2×2 unit cell (containing eight atoms, leading to 24 phonon branches marked by the black dashed lines)[7]. The right panel of figure 5

[6] We note that the use of DFT with purely (semi)local functionals is questionable for use in layered systems where van der Waals forces are expected to play an important role. Nevertheless, the LDA seems to work fine for the calculation of geometries and even of phonon frequencies (however, not for the binding energies) of several layered systems such as graphite [42, 43], hexagonal boron nitride [44], graphene on a nickel(111) surface [41] and MoS_2 [45]. This seemingly good performance is probably due to a fortuitious error cancellation: the small (but non-negligible) covalent part of the inter-layer binding is overestimated while the van der Waals part of the binding energy is completely neglected. For a more precise treatment of van der Waals forces, calculating electron correlation in the random-phase approximation, see the work of Marini *et al* [46] on hBN, Mittendorfer *et al* [47] on graphene bound to metallic substrates or Kim *et al* [48] for the binding of benzene molecules on a Si surface.

[7] There is the eternal question of whether one should use (*ab initio*) optimized lattice constants or experimental lattice constants for the phonon calculations. Since the LDA tends to overbind, the optimized lattice constant is smaller than the experimental one. The calculated phonon frequencies are, in general, a little bit higher than the experimental values and need to be scaled down by about 1% [43]. We use here the experimental lattice constant of pure graphene (for both the isolated graphene and the buffer layer). In this case, the phonon frequencies are a little bit lower than the experimental ones. We thus rescale the calculated phonon dispersions (of both isolated and buffer graphene) by the respective ratio of the experimental and theoretical values of the E_{2g2} (the highest optical mode at Γ) phonon frequencies. For isolated graphene the Raman G-line has the value of 1580 cm^{-1} (according to recent measurements on suspended graphene [49]) and our calculated value is 1568 cm^{-1}. For the buffer layer on SiC(0001), the experimental value (measured by electron energy loss spectroscopy [50]) is 1595 cm^{-1} and our calculated value is 1558 cm^{-1}. These differences are related to the unknown strain state of the buffer layer.

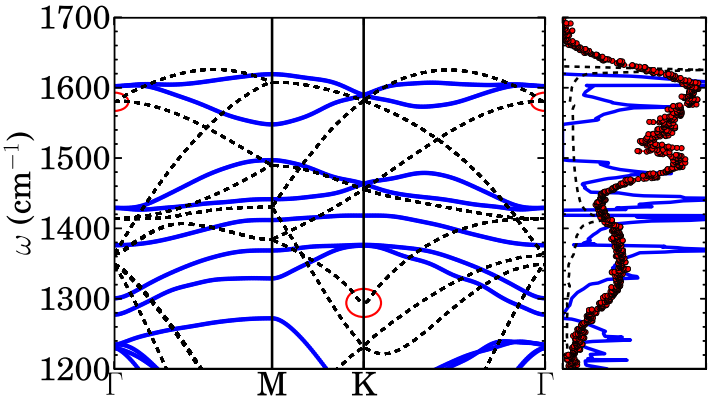

Figure 5. Left panel: phonon modes of the buffer layer (blue lines) and free-standing graphene (black dashed line) in a (2×2) unit cell. The red circles mark the Kohn anomalies at Γ and K of free-standing graphene. Right panel: vDOS of the buffer layer (blue line) and of free-standing graphene (black dashed line) in comparison with the experimental Raman data (red dots).

shows the vDOS of the buffer layer and free-standing graphene, together with the experimental Raman spectra (red dots).

The phonon dispersion of the buffer layer is considerably changed compared to that of isolated graphene. The changes in the electronic structure (lifting of the linear crossing at K and separation of the π and π^* bands by more than 2 eV [26]) lead to the elimination of the Kohn anomalies at K and Γ (marked by red circles in figure 5), similar to the findings for graphene on a Ni(111) surface [41]. A consequence of this is the absence of the 2D line (around 2680 cm^{-1}) in the Raman spectrum of the buffer layer, as seen in figure 3. Furthermore, the buffer layer displays flatter bands than pure graphene. In particular, the overbending of the highest optical branch around Γ almost disappears. This brings the frequency of the highest vDOS peak at 1630 cm^{-1} down to 1620 cm^{-1}, in agreement with the highest peak in the Raman spectrum. Additionally, some degeneracies are broken at the Γ and M points. These modifications lead to noticeable changes in the vDOS of the buffer layer. For instance, a clear gap emerges between 1500 and 1550 cm^{-1}, in agreement with the minimum at the same frequency range in the Raman spectrum. The broad feature in the Raman spectrum around 1355 cm^{-1} can also be associated with peaks in the vDOS of the buffer layer that are due to flat phonon bands. The phonon bands of pure graphene are very dispersive in this range and the corresponding vDOS is flat.

For a better understanding of the gap opening between 1500 and 1550 cm^{-1}, we analyze the phonon eigenvectors of the buffer layer by projecting them onto the eigenvectors of the isolated (undisturbed) graphene. In figure 6, we have projected every eigenvector of the buffer layer onto two subspaces of eigenvectors of isolated graphene. The color of the phonon branch indicates which subspace dominates the character of the vibration. The first subspace (orange color) is composed of the two eigenvectors of highest frequency at the respective phonon-wave vector $\boldsymbol{q}$. This definition becomes ambiguous at the crossing point of the second and third highest modes in between the high-symmetry points. But it is well defined at the high-symmetry points Γ, M and K, where double degeneracies are observed. The second subspace (green color) includes the next four eigenvectors in energy order, and it has also two twofold degeneracies at Γ, M and K. We focus on the dispersion around M. We can assign the first and third phonon

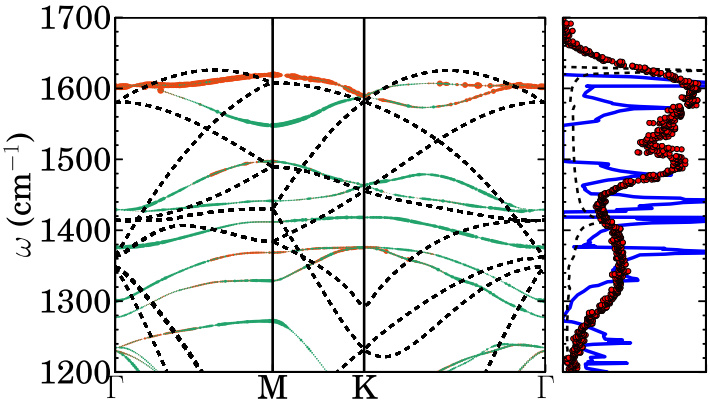

Figure 6. Left panel: phonon bands weighted according to the contribution of two different subspaces (see the main text). Right panel: the same as in figure 5.

branches as being predominantly due to the orange subspace. The frequency difference is $100\,\mathrm{cm}^{-1}$. All the other eigenvectors belong to the green subspace. The perturbation of the buffer-layer vibrations by the partially covalent bonding to the SiC substrate lifts the degeneracies. The splitting is so strong that it even changes the order of the phonon modes: the lower frequency mode due to the first subspace falls below the highest frequency mode of the second subspace. In the phonon dispersion, between Γ and M (and also between Γ and K), this leads to an avoided crossing between the second and third highest phonon modes and thus to the opening of a gap from 1500 to $1550\,\mathrm{cm}^{-1}$. For the lower frequency modes, a similar analysis can be made. But the analysis becomes more complicated due to a large number of participating modes. In the right panel of figure 5, one can observe an approximate agreement between dips in the Raman spectrum and gaps in the vDOS. The same holds for the peaks in the Raman spectrum and in the vDOS. Since we used a simplified supercell for the buffer-layer geometry, we do not expect perfect agreement here. But we consider the present calculation as a qualitative argument that the observed features in the Raman spectra of the buffer layer can indeed be associated with the vDOS.

4. Conclusions

In conclusion, we have been able to identify the Raman spectrum of the buffer layer $(6\sqrt{3})$ which exists at the interface between epitaxial graphene and SiC(0001). We have shown that it constitutes a non-negligible contribution underlying the graphene spectrum, especially at frequencies around the D- and G-line. This implies that a proper Raman analysis of graphene on SiC(0001) requires that the spectrum is also corrected for the buffer layer contributions. Neglecting the buffer layer will lead to errors in the interpretation of Raman spectra of epitaxial graphene on SiC(0001). Furthermore, we have discussed the Raman spectrum of the buffer layer in terms of the vDOS. To this end, *ab initio* calculations on a $(\sqrt{3} \times \sqrt{3})R30^\circ$ superstructure have been performed which revealed a complete extinction of the Kohn anomally, in agreement with the lack of a Dirac cone in the electronic structure [24, 25] and with the absence of a 2D line in the Raman spectrum. As a consequence, phonon bands become flatter than in free-standing graphene. In addition, the carbon–silicon covalent bonds modify substantially the frequencies and lead to a mixing of the phonon branches of isolated graphene. This leads to a breaking of

degeneracies in the phonon dispersion and the vDOS of the buffer layer is richer in structure than that of isolated graphene. In particular, a clear gap between 1500 and 1550 cm^{-1} emerges which agrees fairly well with the Raman spectrum. While there is a qualitative agreement between the calculated vDOS and the Raman spectrum there are also differences, which we believe are due to the simplified model used for the calculations.

Acknowledgments

This work was supported by the European Science Foundation (ESF) in the framework of the EuroGRAPHENE project Graphic-RF (grant number 09-EuroGRAPHENE-FP-018) and by the European Union (EU) in the framework of the project ConceptGraphene (grant number 257829). AMS and LW acknowledge funding from the French National Research Agency (ANR) through project number ANR-09-BLAN-0421-01. Calculations were performed at the IDRIS supercomputing center, Orsay (project number 091827) and at the Tirant Supercomputer of the University of Valencia (group vlc44). The authors thank L Ley, J Ristein and R J Koch for stimulating discussions.

References

[1] Jorio A, Saito R and Dresselhaus M S 2011 *Raman Spectroscopy in Graphene Related Systems* (New York: Wiley)
[2] Ferrari A C *et al* 2006 *Phys. Rev. Lett.* **97** 187401
[3] Graf D, Molitor F, Ensslin K, Stampfer C, Jungen A, Hierold C and Wirtz L 2007 *Nano Lett.* **7** 238
[4] Das A *et al* 2008 *Nature Nanotechnol.* **3** 210
[5] Pimenta M A, Dresselhaus G, Dresselhaus M S, Cancado L G, Jorio A and Saito R 2007 *Phys. Chem. Chem. Phys.* **9** 1276
[6] Gupta A K, Russin T J, Gutierrez H R and Eklund P C 2009 *ACS Nano* **3** 45
[7] Zhang W and Li L-J 2011 *ACS Nano* **5** 3347
[8] Gillen R, Mohr M and Maultzsch J 2010 *Phys. Rev.* B **81** 205426
[9] Gillen R, Mohr M and Maultzsch J 2010 *Phys. Status Solidi* b **247** 2941
[10] Ryu S, Maultzsch J, Han M Y, Kim P and Brus L E 2011 *ACS Nano* **5** 4123
[11] Faugeras C, Nerriere A, Potemski M, Mahmood A, Dujardin E, Berger C and de Heer W A 2008 *Appl. Phys. Lett.* **92** 011914
[12] Röhrl J, Hundhausen M, Emtsev K, Seyller T, Graupner R and Ley L 2008 *Appl. Phys. Lett.* **92** 201918
[13] Ni Z H, Chen W, Fan X F, Kuo J L, Yu T, Wee A T S and Shen Z X 2008 *Phys. Rev.* B **77** 115416
[14] Ferralis N, Maboudian R and Carraro C 2008 *Phys. Rev. Lett.* **101** 156801
[15] Lee D S, Riedl C, Krauss B, von Klitzing K, Starke U and Smet J H 2008 *Nano Lett.* **8** 4320
[16] Robinson J, Puls C, Staley N, Stitt J, Fanton M, Emtsev K, Seyller T and Liu Y 2009 *Nano Lett.* **9** 964
[17] Robinson J *et al* 2009 *Nano Lett.* **9** 2873
[18] Domke K F and Pettinger B 2009 *J. Raman Spectrosc.* **40** 1427
[19] Speck F, Jobst J, Fromm F, Ostler M, Waldmann D, Hundhausen M, Weber H B and Seyller T 2011 *Appl. Phys. Lett.* **99** 122106
[20] Oliveira M H Jr, Schumann T, Ramsteiner M, Lopes J M J and Riechert H 2011 *Appl. Phys. Lett.* **99** 111901
[21] Emtsev K V *et al* 2009 *Nature Mater.* **8** 203
[22] Tiberj A, Camara N, Godignon P and Camassel J 2011 *Nanoscale Res. Lett.* **6** 478
[23] Ferralis N, Maboudian R and Carraro C 2011 *Phys. Rev.* B **83** 081410
[24] Emtsev K V, Seyller T, Speck F, Ley L, Stojanov P, Riley J and Leckey R 2007 *Mater. Sci. Forum* **556–557** 525
[25] VEmtsev K, Speck F, Seyller T, Riley J D and Ley L 2008 *Phys. Rev.* B **77** 155303

[26] Varchon F *et al* 2007 *Phys. Rev. Lett.* **99** 126805
[27] Mattausch A and Pankratov O 2007 *Phys. Rev. Lett.* **99** 076802
[28] Mattausch A and Pankratov O 2007 *Mater. Sci. Forum* **556–557** 693
[29] Mattausch A and Pankratov O 2008 *Phys. Status Solidi* b **245** 1425
[30] Kim S, Ihm J, Choi H J and Son Y-W 2008 *Phys. Rev. Lett.* **100** 176802
[31] Ostler M, Speck F, Gick M and Seyller T 2010 *Phys. Status Solidi* b **247** 2924
[32] Riedl C, Coletti C, Iwasaki T, Zakharov A A and Starke U 2009 *Phys. Rev. Lett.* **103** 246804
[33] Speck F, Ostler M, Röhrl J, Jobst J, Waldmann D, Hundhausen M, Weber H and Seyller T 2010 *Mater. Sci. Forum* **645–648** 629
[34] Forti S, Emtsev K V, Coletti C, Zakharov A A, Riedl C and Starke U 2011 *Phys. Rev.* B **84** 125449
[35] Pankratov O, Hensel S and Bockstedte M 2010 *Phys. Rev.* B **82** 121416
[36] Kohn W and Sham L J 1965 *Phys. Rev.* **140** A1133
[37] Parr R G and Yang W 1989 *Density-Functional Theory of Atoms and Molecules* (Oxford: Oxford University Press)
[38] Giannozzi P *et al* 2009 *J. Phys.: Condens. Matter* **21** 395502
[39] Gonze X and Lee C 1997 *Phys. Rev.* B **55** 10355
[40] Baroni S, de Gironcoli S, Dal Corso A and Giannozzi P 2001 *Rev. Mod. Phys.* **73** 515
[41] Allard A and Wirtz L 2010 *Nano Lett.* **10** 4335
[42] Kresse G, Furthmüller J and Hafner J 1995 *Europhys. Lett.* **32** 729
[43] Wirtz L and Rubio A 2004 *Solid State Commun.* **131** 141
[44] Kern G, Kresse G and Hafner J 1999 *Phys. Rev.* B **59** 8551
[45] Molina-Sánchez A and Wirtz L 2011 *Phys. Rev.* B **84** 155413
[46] Marini A, García-González P and Rubio A 2012 *Phys. Rev. Lett.* **96** 136404
[47] Mittendorfer F, Garhofer A, Redinger J, Klimes J, Harl J and Kresse G 2011 *Phys. Rev.* B **84** 201401
[48] Kim H-J, Tkatchenko A, Cho J-H and Scheffler M 2012 *Phys. Rev.* B **85** 041403
[49] Berciaud S, Ryu S, Brus L E and Heinz T F 2009 *Nano Lett.* **9** 346
[50] Koch R J and Seyller Th *et al* in preparation
[51] Thomsen C and Reich S 2000 *Phys. Rev. Lett.* **85** 5214